5-2022

Enhancing Stability of High-Nickel Cathodes for Lithium-Ion Batteries through Additive Manufacturing of Cathode Structure

Matthew Sullivan

Honors Thesis – Enhancing Stability of High-Nickel Cathodes for Lithium-Ion Batteries through Additive Manufacturing of Cathode Structure

Matthew Sullivan, Dr. Xiangbo Meng

University of Arkansas Honors College, University of Arkansas Department of Mechanical Engineering

Spring 2022 Academic Semester

Abstract:

Lithium-ion batteries (LIBs) are currently the best method to store electrical energy for use in portable electronics and electronic vehicles. New cathode materials for LIBs are consistently studied and researched, but few are as promising and attainable as nickel-rich transition metal oxides such as $LiNi_{1-x-y}Mn_xCo_yO_2$ (NMC). NMC materials exist with many different mass ratios, but higher nickel content materials provide higher energy density. With this increase in capacity comes a sacrifice with cyclability, as high-nickel NMC variants are prone to structure collapse, transition metal dissolution, and cracks due to volume change. In this report, mechanical modification of the electrode by 3D printing is explored as a method to stabilize the cathode structure through optimization of lithiation paths and accommodation of volume change. 3D printed NMC 811 shows substantially higher capacity retention and structure health after cycling at low-rate testing compared with traditional doctor-bladed NMC 811, revealing a scalable and facile method of improving the cyclability of nickel-rich cathode material.

Keywords: Lithium-Ion Battery, 3D Printing, Printed Electrode, Cyclability

1. Introduction:

As the field of lithium-ion batteries (LIBs) has progressed, electrode material with higher energy density has always been highly sought after. Since the inception of LIBs, three main cathode materials have been utilized: Lithium Cobalt Oxide ($LiCoO_2$, LCO) [1], Lithium Iron Phosphate ($LiFePO_4$, LFP) [2], and Lithium Manganese Oxide ($LiMnO_2$, LMO) [3]. All of these cathode materials operate off of the intercalation principle, in which lithium ions are exchanged between interstitial sites in the cathode and anode material during the battery's charge and discharge. Intercalation has been preferred for electrode materials as it is the simplest reaction mechanism and reduces complexities in charging and discharging such as electrode volume change and metal dissolution when compared to other reaction mechanisms such as alloy/de-alloy and conversion [3].

Recently, a new idea and progression towards nickel-rich electrode material has been intensely studied as an intercalation-based electrode reaction. Nickel-rich material offers high energy density, low cost, and low use of rare-earth metals compared with other electrode materials [4]. While the push for higher nickel content increases the energy storage potential of the electrode material, a tradeoff is made with the cyclability of the electrode. Nickel and other transition metals are prone to dissolution into the organic electrolytes used in LIBs, and the internal crystal structure of the material will begin to deteriorate as the battery is continually cycled. Lithium Nickel Manganese Cobalt Oxide ($LiNi_{1-x-y}Mn_xCo_yO_2$, NMC) is the most promising nickel-rich cathode material currently being studied [4]. The atomic ratios of the transition metals - nickel, manganese, and cobalt - are often expressed as a series of numbers following the 'NMC' abbreviation, where NMC 811 will be 80% nickel, 10% manganese, and 10% cobalt. To date, NMC 811 has shown to be the most optimized ratio for energy density and crystal stabilization, but even still it shows

relatively fast decrease in energy storage through its charge cycles. As a result, many researchers have attempted to find methods by which the layered structure of NMC crystals can be preserved and reduce the likelihood of chemical structure collapse into a 3-dimensional spinel structure [5].

Many of the modern methods for preserving the NMC structure have come in the form of surface coatings deposited on the electrode's surface. The most common coating method for NMC electrodes has been using atomic layer deposition (ALD) [6]. ALD is a process by which functional groups on a material's surface are reacted with passing gases to form a stable ionic or covalent coating material [7]. ALD coatings on cathode surfaces in batteries provide additional mechanical support during lithiation and delithiation of a battery while also providing a passive layer between the electrode and electrolyte, reducing transition metal dissolution [8].

In this study, a different method of providing stability on NMC 811 cathode material is analyzed. This study proposes that 3D structuring of the electrode into a complex three-dimensional shape through additive manufacturing (also commonly referred to as 3D printing) may enhance the stability of NMC at both the half-cell and full-cell scale by shortening lithiation paths and optimizing the geometric relationship between the surface area and volume of the electrode.

The rate at which batteries are charged greatly impacts their performance and health [9]. The rate at which current is applied to a battery to charge or discharge is referred to as the 'C' rate, where 1C refers to the amount of time necessary to fully charge or discharge the battery in one hour. This value is dependent on the weight of the electrode, and is expressed relating supplied current in mA/g. While the 'C' rate refers to the amount of charge required to charge the battery in a certain amount of time, it is not as useful in determining the expected health of the electrode structures. For this, areal current density – quantified in mA/cm^2 – is employed. Areal current

density is a key deciding factor in the overall health of a battery. High areal current densities increase the risk of 'mossy' lithium dendrite formation due to lithium dissolution in the electrolyte and unstable solid electrolyte interphase (SEI) formation [11]. These lithium dendrites are completely detrimental to the health of the battery as they run the risk of enhancing lithium dissolution, disrupting the existing layers of SE, and puncturing the separator causing cell short-circuit.

Optimized surface area realized through 3D printing reduces the magnitude of the areal current density and may lead to a healthier battery with higher capacity retention and cycle life. Herein, 3D printing via direct ink writing is demonstrated with NMC 811 electrode material. Slurry synthesis, process optimization, and electrochemical performance results are analyzed.

2. Experimental Methods:

2.1. Traditional Flat-Faced Electrodes:

Traditionally-made NMC 811 electrodes were used as the control sample for this experiment. These electrodes were made by creating a slurry of NMC 811 active material powder (Sigma-Aldrich), carbon black conductivity enhancer (Sigma-Aldrich), and PVDF polymer binder (Sigma-Aldrich) in a 90:5:5 weight ratio in an argon-filled glovebox. The powders were weighed out and transferred into a holding vessel, into which sufficient NMP solvent (Sigma-Aldrich) was added to ensure the slurry could be mixed until homogenous and spreadable. The electrode powders and solvent were mixed in a high-speed mixer at 2000 rpm for 60 minutes, examining the quality of the slurry every 15 minutes to ensure even mixing.

After the slurry was mixed, it was carefully transferred out of the glovebox and spread out over aluminum foil using a 100-micron doctor blade to leave behind an electrode sheet. This sheet

was dried overnight under a low vent until fully dried, and then heated at 100 ℃ overnight until all solvent had been fully evaporated.

The dried flat-face cathodes were then punched into 7/16 inch diameter circles and weighed before being fabricated into coin cells at a mass loading of 3.8 mg/cm^2.

2.2. 3D Structured Electrodes:

The process for synthesizing the slurry for 3D printed NMC 811 cathodes was based off the method demonstrated in Jie Li, et al [10]. The 3D structured electrodes were made using an identical slurry process, with the same 90:5:5 powder ratio as the traditional electrodes. For 3D printed electrodes, the viscosity of the slurry is highly critical. Solutions that were not viscous enough could not hold their shape after being extruded from the printer, creating uneven and unpredictable electrodes, while solutions that were too viscous could not be deposited through extrusion needles fine enough to have high resolution of printing geometry.

The main factor that impacts the viscosity of the slurry is the ratio of solids to liquids in the slurry, represented hereafter as ‘Solids Loading (SL)’ quantified by the weight percentage of solid mass in the powders. Initial tests began at 30% SL, but it was quickly noted that 30% SL was not viscous enough to retain electrode shape upon printing. The SL of the slurries was then increased by 5% with each test up until 60% SL, where it was noted that the slurry required a large sized extrusion orifice to be deposited smoothly. 50% SL gave the ideal viscosity for printing, that allowed for extrusion through a wide range of extrusion needles for high resolution. During the trials, it was also noted that increases in PVDF content above 8% by dry weight were too cohesive to be accurately printed, and often resulted in clumpy or otherwise sticky slurries. PVDF content anywhere below 4% by weight also proved difficult to adhere to the aluminum foil current

collector after drying, resulting in failed electrodes. As such, the ratio of 90:5:5 NMC811:CB:PVDF with 50% SL was optimized for printing.

The printing was carried out on a Hyrel ESR (Engine, Standard Resolution) 3D printer with a Hyrel EMO-25 extrusion head. The 3D model for the printed electrode was prepared using SolidWorks 2020, Student Edition, and was sliced in the printer using the Repetrel Slic3r program.

Slurry was loaded into the main cylinder of the EMO-25 extrusion head with the extrusion-needle adapter and a 0.51 mm needle and fixed into place on the 3D printer. Aluminum foil was placed over the printing bed by spritzing methanol under the foil and using Kimtec wipes to force the foil into place. The print settings were adjusted such that the vertical z-layer of the printer was 0.1 mm and the lateral x- and y-layers were 0.51 mm (the same as the printing needle inner diameter). A movement speed of 25 mm/s was applied to the printer, and a flow rate coefficient of 0.85 was applied to the printing head. These printing settings gave the ideal combination between printer speed, slurry output, and accuracy in printing. The printer bed heater was not utilized, as it was noted that the difference in thermal expansion of the foil and printer bed caused bubbles to form under the foil surface.

A printed electrode sheet made of straight lines was deposited onto the aluminum foil. Each line was modelled to be 0.51 mm thick with a 1.5 mm spacing from centroid to centroid of each line. After the slurry was deposited onto the foil surface, the foil was carefully transferred under a vent to dry overnight before being heated at 100°C and vacuumed for 8 hours to ensure all solvent had been removed from the sample.

The printed sample was weighed before being fabricated into coin cells and a mass loading of 2.46 mg/cm^2.

2.3. Coin Cell Fabrication

The electrodes were fabricated into CR 2032 coin cells (Neware) against a lithium metal anode (source) in an argon-filled glovebox. The electrode sheet (traditional or 3D printed) was punched into a 7/16 inch (~11.1125 mm) diameter circle weighed using a digital scale. The electrode was fixed to the aluminum foil, and so an aluminum foil blank disc was weighed and tared so that it would not factor into the weight of the sample. The cells were assembled against lithium chips cut into a 7/16 inch diameter circle with 20 microliters of 1.2M $LiPF_6$ in 1:1 w/w Ethyl Carbonate : Ethyl Methyl Carbonate electrolyte with a polymer separator (Celgard) The cells were then crimped at ~100 psi using a hydraulic crimper.

3. Electrochemical Testing and Performance:

After fabrication, the cells were rested for 24 hours to ensure proper saturation of the electrodes and electrolyte. The cells were then cycled from 2.7 to 4.3 V at a C/5 current density (C = 200 mA/g) for 500 cycles in a Neware battery cycler. After the cell is fully charged or discharged, there is a ten-minute resting period to allow the electrochemical reaction to finalize and the crystal structures to stabilize before the next exchange of current.

The given charging rate of C/5 is calculated based on the mass of the electrode samples. Importantly, since the mass and surface area of the traditional and the 3D printed electrodes are known or can be mathematically modelled, the areal current density can also be calculated and compared. The mass, area, and mass-normalized current density are all readily available for the traditional flat electrode, and areal current density can easily be quantified:

$$Areal\ Current\ Density = \frac{0.1474\ mA}{0.9699\ cm^2} = 0.152\,\frac{mA}{cm^2}$$

Initially, it may seem daunting to determine the surface area of the printed samples due to their complex geometry and the fact that they can be punched nearly anywhere, resulting in a nearly infinite number of layouts possible. This is not the case, however, as was confirmed using simulation analysis of the printed geometry. Though the nozzle diameter for the printed geometry was 0.51 mm, solid and liquid materials experiencing extrusion inevitably encounter a phenomenon referred to as die swell [12]. Die swell causes the extruded material to expand slightly once the shear stress from the extrusion has been relieved, causing a change in the actual thickness of the extruded geometries.

Analytically, the printed lines measure approximately 1 mm wide, 0.25 mm tall with 1.5 mm spacing. This was modelled using SolidWorks Computer Aided Design software, which has a built-in mass scale. Once the printed sheet was modelled, the initial mass of the model was recorded. Arbitrarily placed holes with the same diameter as the punched sample were removed from the sheet, and the new mass properties were recorded. It was found that due to the symmetry of the print layout and the circular punch, the amount of mass removed from the sample were completely identical, regardless of the location. As such, any layout of printed sample will have the same mass of electrode as confirmed by the simulation and in the recorded mass values from the real samples. Lastly, due to the single-pass printing method using direct ink writing, and the fluid nature of the printed material, the cross section of each line is modelled to be a circular arc curved cross-section with maximum height 0.25 mm and width of 1 mm.

Surface area for this geometry was found by finding the arc length of the surface of the curved lines and multiplying the value by the length of the recorded samples. The areal current density was then found as

$$Areal\ Current\ Density = \frac{0.0984\ mA}{0.7448\ mm^2} = 0.132\frac{mA}{cm^2}$$

for a theoretical reduction in areal capacity of 13.15%. It should be expected, then, that the reduction in areal current density between then printed NMC structure and the traditional NMC structure will improve the capacity retention of the electrode by preserving the health of the NMC layered structure.

4. Results and Discussion:

Health of the cycled traditional and printed cells is analyzed through gravimetric discharge capacity and capacity retention throughout the cycling life. Discharge capacity is received from integrated software and Neware hardware. Capacity retention is determined between the second cycle and the 500th cycle, though it should be noted that the cells are still cycling as of the documentation in this paper. The second charge cycle of the traditional electrode saw a discharge capacity of 0.6126 mAh and the printed sample saw discharge capacity of 0.3983 mAh. The second charge cycle was utilized instead of the first charge cycle because in the first charge cycle, many confounding events occur such as the formation of the initial solid electrolyte interphase layer and crystal structure reorganization due to the induced current and voltage. At the 500th discharge, the traditional electrode saw a discharge capacity of 0.2922 mAh, for capacity retention of 47.70% with a final discharge capacity of 79.19 mAh/g. The printed electrode saw a discharge capacity of

0.2519 mAh for a capacity retention of 63.24% with a final discharge capacity of 102.40 mAh/g.

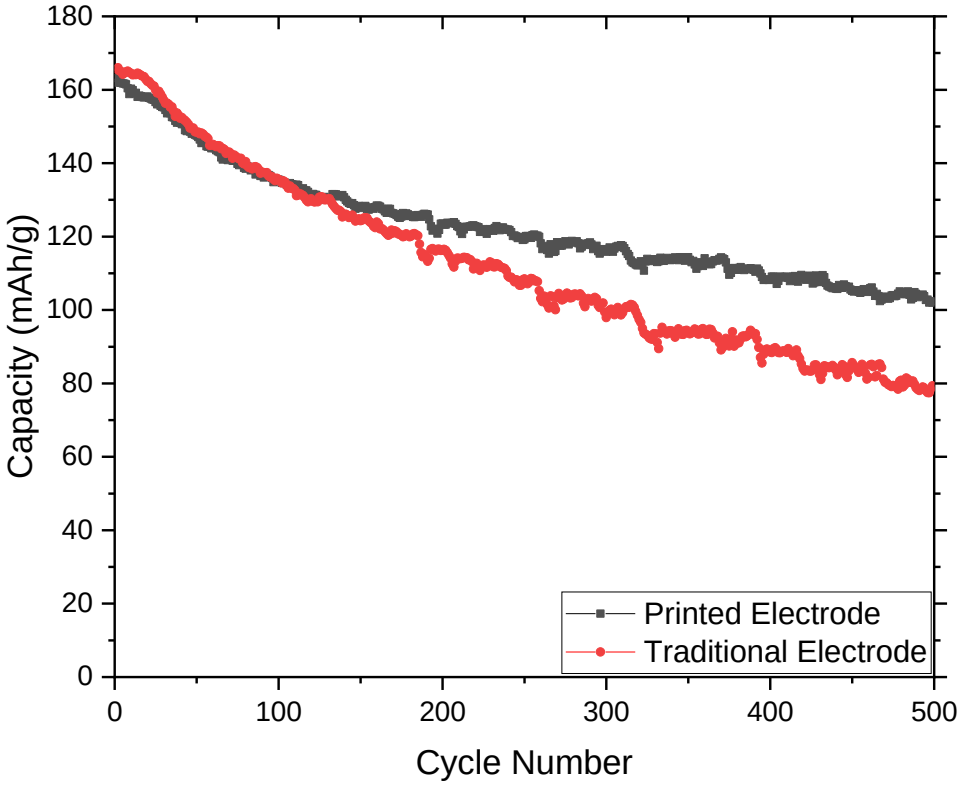

Figure 1: Capacity vs. Cycle Number for Printed Electrode (Gray) and Traditional Electrode (Red)

The traditional electrode initially had a slightly higher capacity of 165.7 mAh/g compared to the printed electrode with 163.1 mAh/g. The traditional electrode quickly began losing capacity after the 10^{th} cycle, however, and eventually dropped below the capacity of the printed electrode just after 100 cycles. From there, the traditional electrode continued to lose capacity at a faster rate when compared with the printed electrode. The increase in capacity retention of the printed cell is likely due to a preservation of the layered structure in NMC due to the decrease in induced stress due to high areal current density. In addition, the shorter path length for lithium diffusion and

higher optimization of surface area may reduce the volume change and strain in the crystal structure during lithiation and delithiation.

After testing, cells of a printed sample and a traditional sample were disassembled to study the morphology change of the electrode during cycling. Images of the electrodes after disassembly are included in Figure 2. It was initially feared that the fabrication of the coin cells may damage the printed structure of the printed NMC, but it appears that the cycling has had minimal effect on the printed structure, as it maintains its initial geometry and definition. Furthermore, it is seen that the lithium metal anode has deformed around the printed structure, verifying that the printed electrode contains sufficient strength to survive the assembly process. On the other hand, the traditional electrode shows signs of cracking and has some sections of the electrode that are missing or disjointed entirely, this may be due to less efficient expansion during cycling, resulting in further oxygen and transition metal loss in the electrode structure.

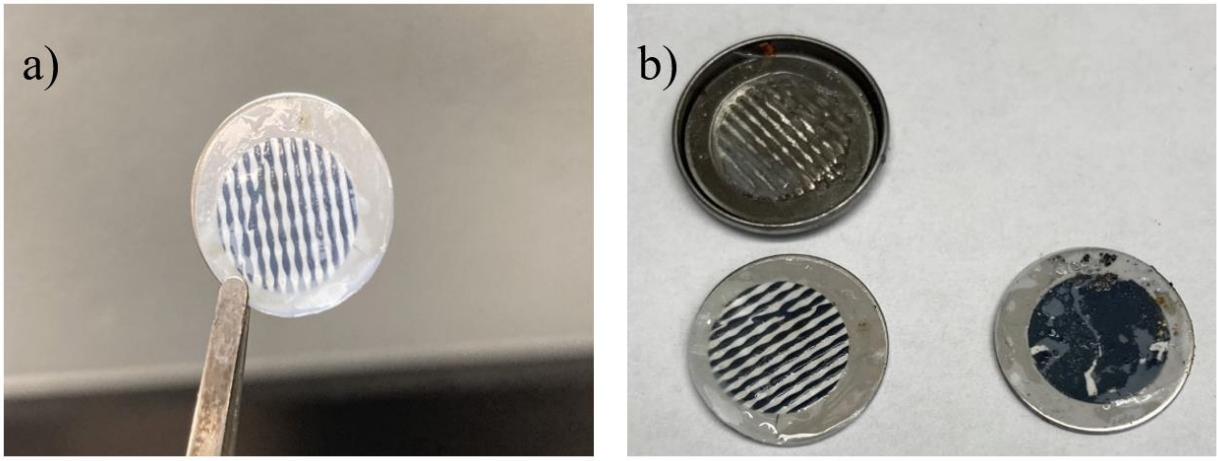

Figure 2: a) Close-up of printed NMC structure after cycling, b) Image of printed NMC electrode (bottom left), lithium metal anode (top left), and traditional electrode (bottom right)

5. Conclusion:

The average difference of 15.54% capacity retention between the printed and traditional cell is not concrete evidence that the printed structure is superior to the traditional structure. Further investigation of the electrode structure via TEM and SEM imaging may prove helpful in determining the health of the secondary crystal structure of the two electrodes. In addition, continuing the cycle the batteries beyond 250 cycles will also aim to create a more complete picture of the effects of printed geometry on capacity retention and chemical stability in NMC 811. As it currently stands, however, the printed NMC811 samples are found to maintain their capacity higher than the traditional NMC811 samples likely because of improved current density and lithiation path optimization.

Furthermore, higher mass-loading with higher density of NMC electrode should also be tested to determine how the performance of printed NMC changes with mass. Higher mass loadings may realize more reliable results, as the effects of volume change coupled with supply of dissolvable materials may change the performance. For further research, a higher density of printed lines, thicker lines, and more pronounced vertical layers should be tested to better understand the relationship between 3D printed performance and mass. After further simple geometries are tested and understood, more complex 3D shapes that take further advantage of surface area and volume ratios can be tested to optimize the performance of printed NMC. Additionally, 3D printing of the NMC electrode lends itself to many other methods by which NMC is stabilized, such as doping and coating. The benefits of both of these techniques may combine as well, to bring NMC 811 closer to commercialization for use in next-generation electronic devices.

Acknowledgements:

Special regards are sent to the University of Arkansas and the University of Arkansas Department of Mechanical Engineering for providing the lab space in which these experiments were conducted. Additional regards are sent to University of Arkansas Honors College for providing additional funding for both the research project and author of this paper. Lastly, a big thank you to the staff of Hyrel 3D Printers for providing the printer and printing accessories at a discounted price and for their assistance in the setup and advanced use of the printer.

References:

1. *Chem. Soc. Rev.*, 2018,47, 6505-6602
2. *J. Mater. Chem. A*, 2016,4, 18210-18222
3. AIP Conference Proceedings 1597, 26 (2014); https://doi.org/10.1063/1.4878478
4. Joris de Hoog, Jean-Marc Timmermans, Daniel Ioan-Stroe, Maciej Swierczynski, Joris Jaguemont, Shovon Goutam, Noshin Omar, Joeri Van Mierlo, Peter Van Den Bossche, Combined cycling and calendar capacity fade modeling of a Nickel-Manganese-Cobalt Oxide Cell with real-life profile validation, Applied Energy, Volume 200, 2017, Pages 47-61, ISSN 0306-2619, https://doi.org/10.1016/j.apenergy.2017.05.018.
5. Haridas, Anulekha & Nguyen, Quan & Song, Botao & Blaser, Rachel & Biswal, Sibani. (2019). ALD-modified LiNi0.33Mn0.33Co0.33O2 (NMC) paired with Macro-Porous Silicon for Li-ion Batteries: An investigation on Li trapping, resistance rise and cycle-life performance. ACS Applied Energy Materials. XXXX. 10.1021/acsaem.9b01728.
6. Mohanty, D., Dahlberg, K., King, D. *et al.* Modification of Ni-Rich FCG NMC and NCA Cathodes by Atomic Layer Deposition: Preventing Surface Phase Transitions for High-Voltage Lithium-Ion Batteries. *Sci Rep* 6, 26532 (2016). https://doi.org/10.1038/srep26532
7. *Chem. Rev.* 2010, 110, 1, 111–131 Publication Date:November 30, 2009
8. Lini Zhao, Guorong Chen, Yuehua Weng, Tingting Yan, Liyi Shi, Zhongxun An, Dengsong Zhang, Precise Al2O3 Coating on LiNi0.5Co0.2Mn0.3O2 by Atomic Layer Deposition Restrains the Shuttle Effect of Transition Metals in Li-Ion Capacitors, Chemical Engineering Journal, Volume 401, 2020, 126138, ISSN 1385-8947, https://doi.org/10.1016/j.cej.2020.126138.
9. Anna Tomaszewska, Zhengyu Chu, Xuning Feng, Simon O'Kane, Xinhua Liu, Jingyi Chen, Chenzhen Ji, Elizabeth Endler, Ruihe Li, Lishuo Liu, Yalun Li, Siqi Zheng, Sebastian Vetterlein, Ming Gao, Jiuyu Du, Michael Parkes, Minggao Ouyang, Monica Marinescu, Gregory Offer, Billy Wu, Lithium-ion battery fast charging: A review, eTransportation, Volume 1, 2019, 100011, ISSN 2590-1168, https://doi.org/10.1016/j.etran.2019.100011.

10. Jie Li, Ming C. Leu, Rahul Panat, Jonghyun Park, A hybrid three-dimensionally structured electrode for lithium-ion batteries via 3D printing, Materials & Design, Volume 119, 2017, Pages 417-424, ISSN 0264-1275, https://doi.org/10.1016/j.matdes.2017.01.088.
11. Andrew Cannon, Emily M. Ryan, Characterizing the Microstructure of Separators in Lithium Batteries and Their Effects on Dendritic Growth, ACS Applied Energy Materials, 10.1021/acsaem.1c00144, (2021).
12. Yuk, Hyunwoo & Zhao, Xuanhe. (2018). 3D Printing: A New 3D Printing Strategy by Harnessing Deformation, Instability, and Fracture of Viscoelastic Inks (Adv. Mater. 6/2018). Advanced Materials. 30. 1870037. 10.1002/adma.201870037.